Forecasting Research

Forecasting Research Division
Scientific Paper No.18

REAL-TIME CORRECTION OF WEATHER RADAR DATA FOR THE EFFECTS OF BRIGHT BAND, RANGE AND OROGRAPHIC GROWTH

by

M Kitchen, R Brown and A G Davies

July 1993

Meteorological Office
London Road
Bracknell
Berkshire
RG12 2SZ
United Kingdom

FORECASTING RESEARCH DIVISION

Scientific Paper No 18

REAL-TIME CORRECTION OF WEATHER RADAR DATA FOR THE EFFECTS OF BRIGHT BAND, RANGE AND OROGRAPHIC GROWTH

by

M Kitchen, R Brown and A G Davies

July 1993

Forecasting Research Division
Meteorological Office
London Road
Bracknell
Berkshire RG12 2SZ
United Kingdom

REAL-TIME CORRECTION OF WEATHER RADAR DATA FOR THE EFFECTS OF BRIGHT BAND, RANGE AND OROGRAPHIC GROWTH

M Kitchen, R Brown and A G Davies
Meteorological Office, Bracknell, U.K.

Abstract

A new method of correcting data from the United Kingdom operational weather radar network is described. The physically-based scheme is designed to produce estimates of instantaneous precipitation rate at the surface by compensating for the effects of the bright band, range and low-level orographic growth. In a preliminary study, the characteristic shape of the vertical profile of reflectivity factor was examined using a climatalogical dataset derived from RHI scans recorded by a high resolution radar. The results were then used to construct an idealized reflectivity factor profile. In the correction procedure, the heights of significant turning points in the profile are diagnosed from relevant meteorological data at each radar pixel. The radar beam power profile is then convoluted with the parametrized profile and the surface precipitation rate found by an iterative method in real-time. The scheme has some important advantages over the alternative correction strategies. Detailed quantitative evaluation in typical cases of mainly frontal rainfall over southern England suggested that RMS errors in estimates of instantaneous precipitation rate over 5km pixels were reduced to less than half compared to the same radar data subject to only a fixed range correction.

1 INTRODUCTION.

Two methods are currently used within the Meteorological Office to derive surface precipitation rate estimates from weather radar data. At the radar sites, a fixed empirical range correction is applied and in addition, at about half the 13 radars in the network, gauge adjustment is performed using the scheme of Collier et al (1983). At the central location where data from the radar network are composited, the radar site corrections may be removed and more sophisticated corrections applied as part of the FRONTIERS rainfall analysis and forecasting system (see Brown et al, 1991). The FRONTIERS corrections are potentially more accurate than the site corrections, but involve human decisions and the output is not as timely; being available some 15 minutes after the data collection time. To achieve reductions in costs and improvements in timeliness, there is now the requirement that corrections must be entirely automatic. This means that the FRONTIERS radar correction scheme cannot continue in its present form.

Recent publications on errors in estimating surface rainfall from weather radar data have suggested that given a correctly calibrated radar, the dominant source of error is due to the radar beam not sampling the precipitation close enough to the ground (Joss and Waldwogel, 1990, Andrieu and Creutin, 1991). Kitchen and Jackson (1993) showed that significant variability (in terms of correcting radar data) in the vertical profile of reflectivity factor occured on the scale of individual pixels. They concluded that for a correction method to have the greatest potential benefit, it should be capable of correcting on a pixel-by-pixel basis (see also Smith, 1990). There appear to be three basic alternative types of radar correction method. These are discussed briefly below, noting in particular their ability to resolve small scale variations in radar errors.

The first group are those which rely on gauge adjustment to resolve and eliminate the differences between radar measurements and surface precipitation rate. Examples of gauge adjustment schemes are numerous but those developed specifically for the UK radars include that of Moore et al (1991), in which data from a dense gauge network is used to generate a field of correction factors which are then applied to subsequent radar data. Collier et al (1983) incorporated knowledge of radar error characteristics into a gauge adjustment scheme by trying to diagnose the likely dominant error in a particular situation and defining appropriate correction domains. Collinge (1991) describes a similar scheme which aims to incorporate orographic growth corrections within gauge adjustment. All gauge adjustment schemes suffer from the problem of random and bias errors introduced by representativeness errors in the comparisons. Another weakness is that economic gauge networks cannot properly resolve the errors associated with a bright band close to the radar, or the spatial detail of orographic enhancement. An advantage is that by relating the radar measurements to measurements of surface precipitation, an attempt is made to deal with all sources of radar errors in a single process, including those due the beam height above the ground, deviation of the Z-R relationship from that assumed, and imperfect radar calibration.

At the other extreme are analytic methods which are aimed at correcting for the beam height above the ground and are based upon analysis of the radar data alone. Examples are by e.g. Koistinen (1991) and Gray (1991), in which an average reflectivity profile is derived by analysing data from several radar beam elevations at ranges up to a few tens of kilometres from the radar. The average profile is then used to correct data from longer ranges. Assumptions of spatial homegeneity are necessary , both in the derivation of the profile and in its application to data at longer ranges. In effect, a correction domain is employed which encompasses the whole area of coverage of a radar, or at least a sector thereof.

Smith (1986) devised an analytic technique for reducing errors due to the bright band which proved very promising in tests. In routine operation however, it was found to be susceptible to large errors when significant variations in the freezing level occured over the area covered by a radar (Gee, 1986). Such variations are common in frontal precipitation in the UK and Harrold et al (1968) described some particularly dramatic examples.

Another difficulty with purely analytic methods is that the profile has to be constructed before any corrections can be applied. They provide no information on how to correct measurements from precipitation areas that are located only at longer ranges from the radar and recourse has to be made to climatalogical profiles.

Calheiros and Zawadski (1987) and Rosenfeld et al (1993) have advocated statistical-physical methods of correction which ensure that the distribution of precipitation rates matches the true distribution on average at all ranges. However, such methods can only operate within a space-

time domain which is sufficiently large that the probability distributions of precipitation rate are reproducible. There main value is in correction of radar data for climatic purposes (Rosenfeld et al, 1993).

The current FRONTIERS range correction represents a hybrid type of method. It is similar to the analytic methods in that reflectivity profiles are used to derive corrections, but all the profiles are idealized and result in a fixed set of corrections (Brown et al, 1991). The choice of correction set and the domain over which it should be applied are made by a human analyst. This approach goes some way to addressing the profile representativeness problem inherent in the purely analytic method and also allows other relevant information such as the type of cloud and its depth to be exploited, albeit indirectly. However, the limited time available to the analyst means that the correction domains are typically of a horizontal scale order 500 km.

It is concluded that the presently available correction methods employ domains which are too large to enable some significant variability in the radar errors to be resolved. The key feature of the new correction method is that the variable parameters in an idealized profile of reflectivity factor are diagnosed *at each pixel* in real-time using relevant meteorological observations. Even if current observations and understanding do not permit the smaller scale variations in the profile to be resolved, such a scheme has the potential for improvement in the future. The method is physically based, in line with the recommendations of Fabry et al (1992), Dalezois and Kouwen (1990) and Austin (1987).

A preliminary study was required to formulate the idealized reflectivity factor profile. High-resolution vertical profiles of reflectivity factor were obtained from the S-band Chilbolton radar operated by the Rutherford Appleton Laboratory. RHI scans from a total of 112 days over a 3 year period were analysed and vertical profiles constructed. The profiles have a resolution of 200m in the vertical and are averages over a 5.3km line in the horizontal. This profile dataset was the same as that used by Kitchen and Jackson (1993) to simulate the range performance of the operational weather radars. In this application, the profiles were used to examine the relationship between the intensity of the bright band and the underlying rainfall rate, the shape of the profile above the bright band, and in a limited investigation of orographic growth at low levels. The results were then combined to form an idealized reflectivity factor profile shape defined by a small number of variable parameters. This preliminary work is described in section 2.

In real-time operation, the radar beam power profile is convoluted with the idealized reflectivity factor profile to calculate the reflectivity factor which should be observed. This is compared with the actual radar measurement and the profile is adjusted in an iterative process until the calculated and measured reflectivity agree to within an acceptable tolerance. More details of the computation and the advantages of the method are discussed in section 3.

The initial validation of the method was by comparing surface rainfall rate estimates from an operational weather radar with near-surface reflectivity factor measurements from an independent radar. This was done to avoid the large representativeness errors that can be associated with radar-gauge comparisons. Differences arising from deviations in the Z-R relationship from that assumed are avoided as well. Also, radar-gauge comparisons are necessarily of rainfall accumulations, rather than instantaneous rates and the comparisons are sensitive to failures by the radar to detect precipitation (Kitchen and Jackson, 1993). The evaluation results are presented in section 4.

Only the basic method and its validation are described here. In the concluding section, some ideas for improvements are outlined.

2 SPECIFICATION OF THE REFLECTIVITY PROFILE.

(a) Profile within the melting layer.

To investigate the relationship between the intensity of the bright band and the reflectivity factor measured in the underlying rainfall, the subset of profiles associated with widespread rainfall from layer-type cloud were first selected. The selection was done on the basis of nearby surface synoptic observations of cloud type and weather.

In highly convective conditions, although a bright band may be present, it is usually less well defined than in more stable conditions because of the strong horizontal gradients in precipitation rate, transient features in the vertical reflectivity profile, and the possible presence of graupel or hail.

The level of the maximum in each reflectivity factor profile was first located. This peak was at first assumed to be due to the bright band and the surface temperature observations were then used to infer an average lapse rate between screen level and the bright band peak. The distribution of lapse rates was then examined to establish quality control limits. All profiles whose lapse rate fell outside the limits were then inspected visually to determine whether to accept the peak as a bright band or not. The reflectivity factor in the rain just beneath the bright band but above any low-level orographic growth is termed the 'background' reflectivity factor and was taken to be the lowest value of reflectivity factor in the three levels up to 800 m beneath the bright band peak.

Fig 1 is a scatter plot showing the observed relationship between the peak bright band reflectivity factor and the background reflectivity factor (in dBZ). These data suggest a slope larger than unity, i.e. the intensity of the peak increase slightly faster than the background. Illingworth (1991), analysed a different Chilbolton dataset which produced a similar result.

Because of the 200m resolution of the reflectivity profiles derived from the Chilbolton RHI data, the magnitude of the peak will have been underestimated on average. The half-power beam-width of the operational radars is 1 deg so the beam is greater than 500m wide for ranges above 30km, i.e. over almost all the area of radar coverage. Thus the details of the shape of the reflectivity factor profile shape and the magnitude of the peak within the bright band are not important for the purpose of correcting the radar data. The most important parameter to define is the area of the peak. The fact that the shape and depth of the bright band was only poorly defined by the 200 m vertical resolution profiles is not too important. The area of the bright band peak was taken to be the area associated with reflectivity factors exceeding the background value. Fig 2 shows a scatter plot of the peak area (A) in mm^6m^{-2}, plotted on a log scale, against the background reflectivity factor (Z_{back}) in dBZ. The correlation coefficient is 0.75 which suggests that more than half the variability in bright band intensity is explained simply by variations in the underlying rainfall. A straight line fitted by eye through these data provides a relationship:-

$$\log A = 1.42 \log Z_{back} + 2.1 \qquad (1)$$

where Z_{back} is now in units of mm^6m^{-3}. The slope in equation 1 being greater than unity is significant for the correction of radar data. Any correction which assumes linear relationship between reflectivity factors measured in the bright band and background values exists may incur significant bias errors, particularly where the ratio is very large.

In the idealized reflectivity factor profile used in the correction method, the bright band is considered to be triangular with a fixed depth of 700m. This depth is probably at the upper end of observed depths (see e.g. Klaassen, 1988, and Illingworth, 1991) but this has the advantage that it reduces the sensitivity of the radar corrections to errors in the assumed height of the bright band, albeit at a small penalty in accuracy when the diagnosed height is correct. Given an assumed background value of reflectivity factor, the area of the peak is estimated from equation 1. This defines the peak reflectivity factor that will produce an idealized bright band of the correct area.

Almost all the operational radars in the UK network operate at C-band, whereas the Chilbolton radar is S-band. In applying results derived from Chilbolton data to the operational network, it is assumed that the wavelength dependence in the reflectivity factor profiles within the bright band are sufficiently small to be ignored. Limited evidence to support this assumption is included in the Appendix.

(b) Profile above the freezing level.

The same sub-set of profiles used to examine the bright band intensity were used to construct an average profile of reflectivity factor above the melting layer. The data were first stratified according to the depth of the snow layer, i.e. the difference between the height of the bright band peak and the height of the top of the precipitation layer. The top was defined as the height of the highest layer in which the average reflectivity factor exceeded $1mm^6m^{-3}$. For each level in the snow layer, the ratio between the reflectivity factor and the background reflectivity factor was calculated and the average ratio over all profiles in each category computed. These average ratios are plotted as a function of height above the bright band peak in Fig 3. Values of the ratio at intervals of 1km were read off these curves and are used to define the profile above the freezing level in the idealized profile.

The shape of the reflectivity profile in the snow layer is extremely variable and the standard deviation of the ratios plotted in Fig 3 was typically of similar magnitude to the ratios themselves. Once the radar beam is mainly within the snow layer, then the corrections will be subject to greater uncertainty (Kitchen and Jackson, 1993). In the future, it may be possible to devise an improved parametrization of the profile in the snow layer. In particular, it is recognised that the profile within convective precipitation may be systematically different from the frontal type precipitation analysed here.

(c) Low-level orographic growth.

Fields of orographic enhancement over the UK were derived by Hill (1983) from case studies of gauge data. The enhancements were specified as a function of wind direction and speed at the 800m level. These enhancement fields have been shown to be of potential benefit to surface precipitation rate estimates, even over the modest topography of southern England (Kitchen and Blackall, 1992). Calculation of the fraction of the enhancement to be added to the radar measurement at each pixel requires knowledge of the growth profile. Hill et al (1981) measured a limited number of profiles recorded over hills in south Wales which showed that most of the growth was confined to the lowest 1.5 km above the ground. They found considerable variations in profile shape between cases despite their rather limited vertical resolution (the radar beam width was of order 1km at ranges of interest).

Within the Chilbolton profile dataset, there are some examples of low-level growth of precipitation and the narrow beam width of this radar provides profiles with better vertical resolution than that available to Hill et al (1981). Fig 4 shows examples of hourly average profiles recorded in two cases analysed by Kitchen (1992). In these two cases, growth was continuous within the rain, with the most rapid increase in reflectivity being below 1.5 km height, in agreement with Hill et al (1981). A few of the profiles show lower growth rates below about 1.0 km , compared to just above. This may reflect the location of the base of feeder cloud.

It is impossible to draw general conclusions about the growth profile shape on the basis of the limited available evidence. In the new correction scheme, the profile was adopted which was simplest computationally, yet consistent with the data in Fig 4. The growth in reflectivity factor is assumed to be linear and commence at 1.5 km above the ground.

(d) The idealized reflectivity factor profile.

Fig 5 shows how the vertical profile of reflectivity is constructed at each pixel. The simplest and most common situations are illustrated. In pixels where no orographic enhancement is diagnosed, the background reflectivity factor defines the reflectivity factor at any point in the profile and also the equivalent surface precipitation rate (Fig 5a). In pixels where orographic enhancement is indicated, there is the additional complication that the fields derived by Hill (1983) are specified in terms of rainfall rate. Thus the background reflectivity factor has first to be converted to an equivalent rainfall rate before adding on the enhancement (Fig 5b). When the surface temperature is below freezing, the profile is defined by assuming linear growth in reflectivity from the inferred precipitation top down to the ground, with any orographic growth superimposed upon this (Fig 5c). The realism of this profile shape, and those adopted in the more complicated situations where a portion of the bright band is within the layer of low-level growth (not illustrated), is not known, but it is hoped to improve the parametrization as observational evidence becomes available. The maximum number of levels used to define the profile is at present 12.

3 THE NEW CORRECTION METHOD.

(a) Outline of the method.

From the previous section, the parameters which define the reflectivity factor profile at each pixel are;

- the background reflectivity factor.
- The height of the freezing level.
- The height of the top of the precipitation layer.
- The magnitude of the anticipated orographic enhancement.

Fixed parameters are;

- The ground height above sea level.

- The radar beam elevation angle (may be the same at all pixels).
- The radar range.
- The radar beam occultation angle.

The height of the freezing level is currently diagnosed from surface synoptic observations. Surface temperature observations within the radar network domain are first analysed to provide values at each radar pixel. A fixed lapse rate is then assumed from the surface up to the freezing level of 6 C km^{-1}; an average value of the saturated adiabatic lapse rate near the ground. However, it was recognised that the freezing level relevant to the melting of precipitation was that of a wet bulb. Accordingly, a recent modification is to calculate the wet bulb freezing level at each observation site and it is this freezing level which is analysed to provide a value at each pixel.

The reliance on surface observations can lead to significant errors in the wet bulb freezing level where precipitation is falling through stable layers such as occur close to warm fronts. However, the effect of errors in height upon the corrections is mitigated by the use of a relatively deep melting layer (see previous section) and the correction method has so far proved very successful at reducing errors due to the bright band.

Hill (1983) specified the orographic enhancement in terms of the wind speed and direction at 800m altitude. Subsequently, he also introduced a humidity scaling factor to reflect the moisture supply into the feeder cloud. The selection of the orographic correction field to be applied at each pixel is based upon an analysis of surface data at present. The observed 10m wind components are analysed to provide an estimate of the 10m wind speed and direction in each pixel. The 800m wind speed and direction is then estimated using a climatalogical correction. There is currently no humidity scaling save the imposition of a humidity threshold. If the analysed surface relative humidity is below the threshold value (currently set at 85%), the orographic correction is set to zero.

Precipitation top height is difficult to define from available observations. In strong convection, precipitation size hydrometeors may extend right up to cloud top whereas in frontal cloud, the cloud depth may be very much larger than the depth of the precipitation layer. Currently, the method uses infra-red images from geostationary satellites combined with radiosonde soundings (if available) to convert the cloud-top temperature to an equivalent height. This height is then assumed to be the top of the precipitation layer except in two circumstances. If the top of the precipitation is diagnosed to be at a height of less than 1.5 km, then significant precipitation is considered highly unlikely and 1.5 km is adopted as the minimum. A situation which typically occurs in wintertime warm fronts is where the freezing level is very low with very cold cirrus cloud extending well above the main frontal precipitating cloud layers. In such conditions, precipitation development is not associated with the observed cloud top but much closer to the freezing level. Some correction for range is normally required in these conditions and to ensure that some is applied, the precipitation top in the idealized profile is limited to being no more than 4km above the freezing level.

These three aforementioned variable quantities are required over the whole of the area covered by the present UK radar network (approx 500 x 1000km).

As the intensity of the bright band is not directly proportional to the background reflectivity factor, an iterative method is required to derive a surface rainfall rate estimate from the measured reflectivity. An intermediate value of the background reflectivity factor is first selected (currently

200 mm^6m^{-1}) and the reflectivity factor profile constructed. The beam power profile is convoluted with the reflectivity factor profile to calculate what reflectivity factor the radar would measure ($\overline{Z}$) using the following equations (from Brown et al., 1991).

$$\overline{Z} = \int_{\alpha}^{\beta} Z(\phi) f(\phi) d\phi \tag{2}$$

where ϕ is the elevation angle, $f(\phi)$ is the fraction of the radar beam power in the range ϕ to $\phi + d\phi$ and the beam power is negligible outside the range of angles α to β.

$$f(\phi)d\phi = [P(\phi)d\phi] / \int_{\alpha}^{\beta} P(\phi)d\phi \tag{3}$$

and $P(\phi)d\phi$ is the relative power returned from angles in the range ϕ to $\phi + d\phi$. The transmitted beam power profile relative to the beam center ($\phi = 0$) specified by the radar manufacturer is well fitted by the function $[\sin(k\phi)/k\phi]^2$ (Brown, 1987), where k is a constant (=159.46 for ϕ in degrees). The function falls to zero for $|\phi| > 1.13^o$ and the power is assumed to be zero outside this range. The half-power beam width is 1^o. Therefore the received power profile is given by:-

$$P(\phi) = [\sin(k\phi)/k\phi]^4 \tag{4}$$

$\overline{Z}$ is found by integration of equation 2 using 0.03^o angular increments. α is the radar horizon at a particular azimuth, which is constructed from a combination of a site survey and analysis of a high resolution topographic map. Refraction of the radar beam was taken into account using the '4/3rds earth' correction.

In general, the calculated reflectivity factor will not equal that which was measured and so the integration is repeated using different values of the background reflectivity factor until a value is found which when used to define the profile, results in agreement between calculated and measured reflectivities to within some tolerance. The value of the fractional tolerance adopted is 0.1. Using a very simple iteration method, convergence is normally achieved within about 10 iterations. The reflectivity factor at ground level associated with this background reflectivity is then translated into rainfall rate using the assumed $Z - R$ relationship ($Z = 200R^{1.6}$).

In two sets of circumstances, the iteration is halted for the reasons discussed below. Firstly, if the orographic correction is too large, the calculated reflectivity factor may exceed the measured reflectivity factor even for an assumed background reflectivity factor of zero. Such occurrences are inevitable because the orographic corrections are additive and will also be subject to some uncertainty. If, for this reason, no convergence is achieved after 20 iterations, the orographic corrections are reduced by the ratio of the measured reflectivity factor to the minimum calculated reflectivity factor. This solution is not entirely satisfactory since the problem will only be encountered where the radar beam intercepts a significant part of the orographic growth. Thus orographic corrections will be reduced on occasion close to the radars but never at long range. A better solution is mentioned in the concluding section.

Secondly, if the height of the top of the precipitation is underestimated, and the radar beam is assumed wrongly to be just grazing the top of the precipitation layer, the result is an unrealistically large value of the background reflectivity factor. This is prevented by imposing a maximum background reflectivity factor equivalent to a rainfall rate of $64mmh^{-1}$; the iteration is halted if this

value is exceeded. Also, the estimated surface rainfall rate is limited to no more than ten times the measured rainfall rate.

Kitchen and Jackson (1993) showed that the main cause of underestimation of surface precipitation accumulations at long range in wintertime was the failure of the radar to detect precipitation, rather than simple underestimation of the rainfall rate. The new correction method provides an assessment of the radars ability to detect precipitation in each pixel based upon the diagnosed precipitation depth and freezing level height. At those pixels within radar range where no precipitation is detected, vertical profiles of reflectivity factor are constructed in exactly the same way as at 'wet' pixels. A fixed value of the background reflectivity factor, termed ' the detection threshold', is assumed and the reflectivity factor that would be measured by the radar computed. If this calculated reflectivity factor is greater than the minimum that should be detectable by the radar, then this pixel is considered to be within the detection area for this value of the threshold. The minimum detectable reflectivity for the radar can be taken from the manufacturer's specification. The minimum acceptable signal in an individual 1^o x 187.5 m polar cell is set at a value of $\overline{Z}$ equivalent to a rainfall rate of 0.125 mm h^{-1} at a range of 100 km ($\equiv$ 7.2 mm^6 m^{-3}). If a single polar cell within a 5 km pixel has a measured reflectivity above the threshold, and the average reflectivity over the pixel is equivalent to a rainfall rate $>$ 0.031 mm h^{-1}, then the radar should record precipitation. The effective limit of detection (denoted by Z_{min}) was taken to be the higher figure, 7.2 mm^6 m^{-3}, to provide a conservative view of the radars ability to detect precipitation. At ranges $<$ 100 km, range-dependent attenuation of the received signals is applied, and the limit is therefore constant over this range. For ranges $>$ 100 km, the detection limit will increase with the square of the range, i.e., $Z_{min}(r > 100 \text{ km}) = (r^2/100^2)Z_{min}(r = 100)$. In the current version of the correction scheme, detection areas are computed for two detection thresholds; $0.125 mm h^{-1}$ and $1.0 mm h^{-1}$. The detection areas will be useful initially in deciding how to merge precipitation diagnosed from satellite data with the radar data in a combined precipitation analysis.

It is intended that, in operational use, the correction method will be applied to data from each radar in the network separately. A composite image of the data from the network will then be formed from these corrected data.

(b) Advantages of the method.

The rationale behind the method was explained in the introduction. Having described the method in more detail, some of the particular advantages can now be listed.

- The basic orographic enhancement fields devised by Hill (1983) can be utilised as they stand.
- The method can exploit a wide range of meteorological information from conventional observations and forecast models to derive the reflectivity factor profile. This should be advantageous compared to methods which attempt to derive the profile analytically from radar data alone. Also, the use of an idealized profile shape precludes the possibility of deriving corrections based upon spurious, unrepresentative, profiles which may result from purely analytic methods.
- The requirement for human intervention that was a feature of the FRONTIERS radar corrections has been removed, resulting in considerable cost savings.

- There is the potential for resolving the small scale variability in reflectivity profiles. This is the main advantage over correction methods which assume uniform profile shape over large domains, although current limitations in understanding and diagnosis of reflectivity factor profile variations may not allow this potential to be realised at present. As the resolution of both observations and models increases, the accuracy of fields of freezing level height and the precipitation depth should increase. Any improvements will feed through directly into improved surface precipitation estimates without any substantial changes to the method. Similarly, the reflectivity factor profile shape could be refined as a result of new research.
- The method is almost entirely physically based. Only two features have been introduced purely as quality control; the limitation of the range correction factor to no more than ten and the overall limitation on precipitation depth above the freezing level.
- The method can generate useful diagnostic products, namely the detection areas and the indication of errors in the orographic correction fields which are both discussed above.

The main disadvantage of the method is the computer processing power required for the iterative convolution of the beam power profile with the reflectivity factor profile in real-time. Indeed, without recent dramatic increases in processing speed available in workstations, the method would probably not be practical for real-time use. The lack of gauge adjustment also requires the radar to be correctly calibrated.

4 INITIAL EVALUATION OF THE METHOD.

RHI data from the Chilbolton radar collected during February and March 1991 were used in the initial evaluation of the method. Note that this Chilbolton dataset was completely separate from that used in the development phase. During this period, the Chilbolton radar executed series of RHI scans along 24 regularly spaced azimuth angles and data from ranges up to about 60km were considered for comparison purposes. For 7 wet days during the two months, the data from the Wardon Hill operational radar were corrected using the new method in a realistic simulation of operational conditions. Data from Chilbolton RHI scans within each pixel were grouped into height bands 200m deep. The 5km pixel data from Wardon Hill were then compared with collocated Chilbolton reflectivity factors for the layer centred at 500m. The 500m reflectivity factor was taken to be the best estimate of the true surface precipitation rate. All reflectivity factor profiles were subject to quality control to ensure that there was adequate data from the 500m level and to minimise contamination by ground clutter or occultation. Comparisons were also rejected from within a range of azimuths from Wardon Hill within which the Wardon Hill radar suffers from severe occultation. The comparison pixels were at ranges between 40 and 125 km from Wardon Hill, i.e. at ranges typical of the operational network coverage of the UK land area. Data were considered to be collocated if both radars sampled the same pixel within two minutes of each other. In two minutes, the spatial pattern of rainfall may be expected to be displaced by no more than half a pixel width at typical advection speeds.

Checks were made to ensure that radar calibration errors did not introduce bias errors into the comparison and also to estimate the true elevation angles of the Wardon Hill radar beams for use in the correction procedure. Details of these tests are include in the Appendix.

Reflectivity factor measurements by both radars were converted to equivalent rainfall rate using the standard $Z - R$ relationship. The RMS difference for these comparisons therefore probably underestimates the total error associated with the correction method as variations in the Z-R relationship are excluded. However, at the radar ranges represented here, errors due to beam height above the surface probably dominate those due to Z-R variations.

The representativeness errors associated with the use of line average reflectivity factors as an estimate of areal averages over the 5km pixels was quantified as follows. A number of pixels close to the Chilbolton radar were intersected by RHI scans along two or three adjacent azimuths. The line average reflectivity factors at the 500m level within these pixels were computed for each scan. Using exactly the same collocation criteria as for the comparison between the radars, the RMS difference between the equivalent precipitation rates measured within the same pixel were computed for each case. The representativeness error (ε) associated with the Chilbolton line averages was then taken to be the square root of half the mean square difference. To provide a conservative estimate of the representativeness errors, and to avoid a few anomalously large differences contaminating the result, all comparison differences more than three times the initial RMS difference were excluded and the representativeness error recomputed. All the statistics are of differences in precipitation rates, rather than the log ratios frequently used in radar/gauge comparisons. This is because the main use of the quantitative radar data is in flood forecasting, where interest is mainly in high accumulations. Log ratio statistics tend to be dominated by the lower precipitation rates in widespread frontal rainfall. The disadvantage of simple differences is that in some cases, they are clearly not normally distributed, particularly for raw data subject to large bright band overestimation where the difference distribution is skewed.

Most of the cases were of typical, mainly light, wintertime frontal precipitation (see Table 1). Results from all the cases analysed which yielded a reasonable number of collocations have been included. At the ranges where the comparisons were made, the Wardon Hill radar beam used for operational precipitation measurements (0.25deg elevation) frequently intercepted the melting layer and in most cases, radar errors were dominated by the bright band in the comparison area. To include some tests where the beam centre was above the melting layer; in selected cases, the method was also applied to data from beams of higher elevation (0.75 and 1.25deg). At 100km range, the 0.75 deg beam centre is at approximately the same height as the 0.25 deg beam is at 150km range.

Examples of the comparisons are shown in Figs. 6 and 7 where the corrected data may be compared with that for the 'raw' radar data. The 'raw' data are as received from the radar site. They are not strictly raw data since a simple occultation correction, an empirical range correction and an attenuation correction are all applied at the radar site. The effects of the first two site corrections were removed prior to the new correction scheme being applied. These scatter plots demonstrate the effectiveness of new method in reducing the large bright band errors present in the raw data.

The comparison statistics for each of the cases are presented in Table 2. In the table, N is the number of satisfactory collocations, C denotes the surface precipitation rate estimate derived from Chilbolton data and R is the surface precipitation rate estimate from the Wardon Hill data. The correction method consistently reduced the RMS difference RMS C-R compared to raw data. The mean differences, whether overestimation due to bright band or underestimation due to the effects of orographic growth or beam overshooting, were also reduced in almost all cases.

The best estimate of the true errors in the surface precipitation rate estimates were computed

by subtracting ϵ^2 from the mean square comparison differences. In most cases, the impact of representativeness errors upon the error estimates was small; confirming one advantage of verification against radar rather than gauge data. In the last two cases in Table 2 however, the residual RMS errors were of comparable magnitude to ϵ. In these cases, the RMS error estimates are more uncertain, particularly in view of the non-normal difference distributions.

The RMS errors are plotted in Fig 8 as a function of the mean precipitation rate in each case. The largest improvements tended to result from the higher rainfall rate cases where the bright band is more intense. For low precipitation rates subject to small errors, the relative improvement was much smaller. For the $0.25deg$ elevation beam, the corrections confined RMS errors to $< 0.5mmh^{-1}$ despite RMS errors in the raw data of up to $1.39mmh^{-1}$. The percentage reduction in RMS error for each case varied from 10-78%.

Raw data from 1.25deg elevation beam in the 21st Feb case seriously underestimated the surface precipitation rate (mean $C - R = -0.44mmh^{-1}$). The correction procedure was very successful in eliminating the range effect in this case. It was less successful with another case of smaller underestimation in the 0.75deg beam on the 27th Feb. Similarly, the range corrections proved too small in the 7th Feb case of shallow snow showers. It is to be expected that once the beam centre is within the snow layer, the performance of the corrections will be rather variable, given the observed diversity in reflectivity factor profile shape noted in section 2.

Statistics computed over all 7 cases for the lowest elevation beam (0.25 deg), suggest that the corrections achieved a reduction of about 60% in the RMS error overall (Table 3).

It should be emphasised that these results pertain to unremarkable cases of generally light frontal rainfall in which RMS errors in the raw radar data are of the same order as the mean surface precipitation rate. The expectation is that larger relative reductions in error can be achieved in heavier rainfall cases with, for example, intense bright band contamination.

5 CONCLUSIONS AND FURTHER DEVELOPMENT.

A new method of estimating surface precipitation rates from radar data has been proposed. The method corrects for the effects of the variations in the vertical profile of reflectivity and thus is designed to compensate for the effects of bright band, range, and orographic growth. The key feature is the ability to use a different reflectivity factor profile at each pixel which gives the method the potential for resolving small scale variations in the profile ignored by other methods. The method has been shown to be capable of practical implementation and particularly successful in reducing errors due to the bright band. In 7 cases of typical wintertime rainfall over southern England, the scheme achieved a reduction of 63% in the RMS error in equivalent surface precipitation rates when compared to the raw radar data subject only to a fixed range correction. As a major operational use of the radar data is in flood forecasting, it is encouraging that the evaluation experiment indicated that the biggest gains in accuracy were achieved in cases of higher rainfall. However, the verification requires extending to a greater range of synoptic types including flood cases. This work is now in progress.

It is planned to implement the correction scheme in a new Meteorological Office short period precipitation analysis and forecasting system. In the meantime, some areas for further development have been identified. Systematic errors can arise from the difficulty in diagnosis of the precipitation

depth and/or variations in the profile of reflectivity factor within the snow layer. The data from the higher elevation radar beams contains some information on the reflectivity factor profile, albeit of low vertical resolution. This could be used to refine the diagnosed vertical reflectivity factor profile by ensuring that the profile is consistent with the radar measurements from two or more beams. Practical implementation of this idea would require extending the iteration to two or more dimensions so clear benefits would need to be achieved in order to justify the additional complexity.

The wet-bulb freezing level height derived from the Meteorolgical Office mesoscale numerical weather prediction model could also be superior to that derived from surface observations. The greatest benefit could arise if the model representation of the vertical structure is realistic in warm-front situations where the frontal surface is beneath the melting layer.

As mentioned in the introduction, the scheme relies at present upon accurate radar calibration being maintained. Also, there is the assumption of a fixed Z-R relationship which may introduce systematic biases into the results in some cases. To compensate for possible drifts in radar sensitivity and changes in the Z-R relationship, it may be advantageous to incorporate some form of gauge adjustment into the method. This is not straightforward because the relationship between the background reflectivity factor and the calculated measured reflectivity factor is non-linear and the gauge accumulation must be compared with an integration of several radar measurements which are dissimilar in general. At the pixels within which lie the adjustment gauges, the correction procedure would need to be applied iteratively. An assumed radar 'sensitivity' would be varied until satisfactory agreement was obtained between the gauge accumulation and integrated radar surface estimates. The radar sensitivity at each gauge pixel could then be averaged in some way to form an overall assessment factor. The radar data field would then be multiplied by the assessment factors and then the correction scheme could procede normally.

Regarding the orographic corrections, in the near future, it is hoped to use wind data from the mesoscale numerical model to select the orographic correction field to be applied at each pixel. The feedback between the correction scheme and the choice of orographic correction field requires improvement. One idea is to examine the occurrence of the condition of non-convergence caused by the corrections being too large over some defined upland area. If the number of affected pixels is judged to be significant, then the orographic correction fields applied over this area should be revised. Further observational studies of the reflectivity factor profile in enhancement conditions may also help to improve the profile parametrization.

6 APPENDIX

The results from the correction method are sensitive to errors in radar beam elevation angle of order a few tenths of a degree. It was recognised that true beam elevations may be significantly different from the nominal angles which correspond to the geometric alignment of the antenna. To establish the true elevation angles for the Wardon Hill radar, some direct comparisons were made with the Chilbolton radar. Vertical profiles of reflectivity factor within selected pixels derived from Chilbolton RHI scans were convoluted with the Wardon Hill beam power profile to simulate the measurements from the Wardon Hill radar. The method is described in detail in Kitchen and Jackson (1993). The simulations were repeated assuming different Wardon Hill beam elevation angles around the nominal values. Fig A1 shows the results from three different case studies where

a well defined minimum in the RMS difference between the Wardon Hill measurements and the Chilbolton simulations was observed. In each case, the minimum was the result of assuming that the Wardon Hill radar beams were about 0.25deg lower than the nominal angles. The lower angles were therefore used in the correction of all Wardon Hill data used in the evaluation exercise. Fig A2 is an example of one of many direct comparison scatter plots from the cases in Table 1. There was no evidence of significant systematic differences between the radars and radar calibration errors are unlikely to have contributed significantly to the observed differences reported in section 4. Some of the higher equivalent rainfall rates in Fig A2 arise from the beam intercepting the bright band. The lack of systematic differences at these higher rates is an indication that any wavelength dependence of the reflectivity factor within the bright band was small enough to be ignored in the formulation of the corrections.

7 ACKNOWLEDGEMENTS.

The Chilbolton radar data were provided by the Radio Communications Research Unit of the Rutherford Appleton Laboratory. John Goddard and Kevin Morgan of the Rutherford Appleton Laboratory provided advice on its processing.

8 REFERENCES.

Andrieu, H. and Creutin, J. D. 1991 Effect of the vertical profile of reflectivity on the rain rate assessment at ground level. Preprints 25th Int. Conf. on Radar Meteorology, Paris. Amer. Meteor. Soc., 832-835.

Austin, P. M. 1987 Relation between measured radar reflectivity and surface rainfall. Mon. Wea. Rev.,115, 1053-1070.

Brown, R. 1987 The definition of the radar beam power profile. Nowcasting Group Technical Note No 17, Meteorological Office, Bracknell, Berks.

Brown, R., Sargent, G.P. and Blackall, R. M. 1991 Range and orographic corrections for use in real-time radar data analysis. Hydrological applications of weather radar. Eds I. D. Cluckie and C. G. Collier, published by Ellis Horwood, Chichester, 219-228.

Calheiros, R. V. and Zawadski, I. 1987 Reflectivity-rain rate relationships for radar hydrology in Brazil. J. Climate and Appl. Meteor.,26,118-132.

Collier, C. G., Larke, P.R. and May, B.R. 1983 A weather radar correction procedure for real-time estimation of surface rainfall. Quart. J. Roy. Meteor. Soc., 109, 589-608.

Collinge, V.K. 1991 Weather radar calibration in real time - prospects for improvement. Hydrological applications of weather radar. Eds I. D. Cluckie and C. G. Collier, published by Ellis Horwood, Chichester, 25-42.

Dalezois, N. R., and Kouwen, N. 1990 Radar signal interpretation in warm season rainstorms. Nordic Hydrology, 21, 47-64.

Fabry, F., Austin, G. L. and Tees, D. 1992 The accuracy of rainfall estimates by radar as a function of range. Quart. J. Roy. Meteor. Soc., 118, 435-453.

Gee, G. 1986 Four case studies illustrating some deficiencies of the bright band correction procedure.

Nowcasting Research Group report No 6, Meteorological Office, Bracknell, Berks.

Gray, W. 1991 Vertical profile corrections based on EOF analysis of operational data. Preprints, 25th Int. Conf. on Radar Meteorology, Paris. Amer. Meteor. Soc., 821-823.

Harrold, T. W., Browning, K. A. and Nicholls, J. M. 1968 Rapid changes in the height of the melting layer. Met. Mag., 97, 327-332.

Hill, F. F. 1983 The use of annual average rainfall to derive estimates of orographic enhancement over England and Wales for different wind directions. J. Clim.,3, 113-129.

Hill, F. F., Browning, K. A. and Bader, M. J. 1981 Radar and raingauge observations of orographic rain over south Wales. Quart. J. Roy. Meteor. S. 107, 643-670.

Illingworth, A. J. 1991 Assessment of radar bright band correction procedures. Unpublished report prepared for the Meteorological Office.

Joss, J. and Waldvogel, A. 1990 Precipitation measurements and hydrology. In Radar in meteorology, Ed. D Atlas. Batten Memorial and 40th Radar Meteorology Conference. American Met. Soc., 577-606.

Kitchen, M. and Blackall, R. M. 1992 Orographic rainfall over low hills and associated corrections to radar measurements. J. Hydrol., 139, 115-134.

Kitchen, M. and Brown, P. M. 1992 Correction of radar measurements for orographic growth beneath the beam. Proc. 2nd Int. Symposium on Hydrological Applications of Weather Radar. Univ. of Hannover, 1992.

Kitchen, M. and Jackson, P. M. 1993 Weather radar performance at long range - simulated and observed. J. Appl. Meteor., 32, 975-985.

Klaassen, W. 1988 Radar observations and simulation of the melting

layer of precipitation. J. Appl. Meteor., 45, 3741-3753.

Koistinen, J. 1991 Operational correction of radar rainfall errors due to the vertical reflectivity profile. Preprints, 25th Int. Conf. on Radar Meteorology, Paris, 1991, Amer. Meteor. Soc., 91-94.\\

Moore, R. J., Watson,B.C., Jones,D.A. and Black, K. B. 1991 Local recalibration of weather radar. Hyrdrological applications of weather radar. Eds I. D. Cluckie and C. G. Collier, published by Ellis Horwood, Chichester, 65-73.

Rosenfeld, D., Wolff, D.B. and Atlas,D. 1993 General probability-matched relations between radar reflectivity and rain rate. J. Appl. Meteor., 32, 50-72.

Smith, C. J. 1986 The reduction of errors caused by bright bands in quantitative rainfall measurements using radar. J. Atmos. Ocean. Technology, 3, 129-141.

Smith, P. L. 1990 Precipitation measurement and hydrology: Panel Report. In: Radar in meteorology, Ed. D. Atlas. Batten Memorial and 40th Radar Meteorology Conference. American Met. Soc., 607-618.

9 Tables and Figure Captions.

TABLE 1. SYNOPTIC CONDITIONS DURING THE CASE STUDIES.

Date (1991)	Time period (UTC)	Synoptic conditions
7 Feb	0500-1000	snow showers
21 Feb	1500-1800	warm sector
22 Feb	1400-2000	warm front/sector
27 Feb	1600-1900	weak fronts
8 Mar	0000-0500	warm front/sector
16 Mar	1100-1530	cold front
18 Mar	1200-2300	warm front

TABLE 2. EVALUATION RESULTS.

Date (1991)	N	elev (deg)	mean C (mm/h)	E (mm/h)	mean (C-R) raw (mm/h)	mean (C-R) corr (mm/h)	RMS (C-R) raw (mm/h)	RMS (C-R) corr (mm/h)	RMS error raw (mm/h)	RMS error corr (mm/h)	reduc (%)
7 Feb	15	0.25	0.27	0.02	-0.17	-0.12	0.28	0.25	0.28	0.25	13
21 Feb	63	0.25	0.70	0.16	0.47	0.09	0.85	0.32	0.83	0.28	67
21 Feb	62	0.75	0.71	0.16	0.15	0.23	0.71	0.51	0.69	0.48	31
21 Feb	46	1.25	0.80	0.16	-0.44	-0.01	0.61	0.37	0.58	0.34	42
22 Feb	136	0.25	0.94	0.18	0.18	-0.10	0.92	0.47	0.91	0.44	52
22 Feb	135	0.75	0.95	0.18	0.16	0.11	1.04	0.60	1.02	0.58	44
27 Feb	43	0.25	0.56	0.06	0.10	-0.08	0.29	0.19	0.28	0.18	36
27 Feb	43	0.75	0.57	0.06	-0.19	-0.13	0.29	0.22	0.28	0.21	26
8 Mar	95	0.25	0.57	0.19	0.17	-0.05	0.54	0.28	0.51	0.21	58
16 Mar	84	0.25	1.04	0.52	0.48	0.00	1.49	0.60	1.39	0.30	78
16 Mar	84	0.75	1.04	0.52	1.28	0.31	2.85	0.93	2.80	0.77	72
18 Mar	148	0.25	0.46	0.17	-0.07	-0.07	0.24	0.23	0.17	0.16	10

Results of comparison between surface precipitation rate estimates from Wardon Hill data and verification from the Chilbolton radar. The 7 case study periods are those listed in Table 1.

TABLE 3. EVALUATION STATISTICS COMPUTED OVER ALL CASES.

	Raw (mm/h)	Corrected (mm/h)	Reduction (%)
mean C-R	0.18	-0.05	71
RMS C-R	0.82	0.38	53
RMS error	0.78	0.29	63

Computed using data from Wardon Hill 0.25 deg elevation beam only;
584 individual comparisons.

Figure 1. Scatter plot showing the relationship between the peak reflectivity factor measured in the bright band and the reflectivity factor in the rain beneath the bright band (the 'background' reflectivity factor, defined in the text). The data are from 1524 profiles of reflectivity factor recorded in widespread precipitation from stratiform cloud.

Figure 2. The area of the bright band peak as a function of the background reflectivity factor. The profile dataset was the same as that used in Fig 1.

Figure 3. Results of analysis of reflectivity profiles within the snow above the melting layer. The reflectivity profiles were grouped into bands according to the separation distance between the height of the bright band peak and the top of the precipitation layer. The closed triangles are for separations 4-5km; the open circles, 3-4km; the closed circles, 2-3km; the open squares, 1-2km and the open triangles, 0-1km. The points on the curves represent the average ratio between the measured reflectivity factor at that level to the background reflectivity factor.

Figure 4. Hourly average reflectivity factor profiles recorded in two cases with low-level growth of precipitation; a) 20th Oct 1989 and b) 19th Oct 1989. The dashed portion of each profile is where the bright band peak has been omitted for clarity. The numbers at the base of each profile indicate the averaging period (UTC).

Figure 5. Examples of the construction of the idealized reflectivity factor profiles used in the correction method. a) is the most common case where no low-level orographic growth is diagnosed and the melting layer is within the precipitation layer. b) is similar to a) but with orographic growth. c) shows the simplified profile adopted when the surface temperature is less than 0 deg C and the precipitation is assumed to be snow.

Figure 6. Example of the results of comparison between collocated measurements of instantaneous precipitation rate by the Wardon Hill operational weather radar and near-surface precipitation rate estimates derived from Chilbolton radar RHI data within the same 5km pixels. The time period for the comparison was 1500-1800UTC on 21 Feb 1991. a) is for the 'raw' Wardon Hill data and b) is for the same data corrected using the new method. In this case of typical wintertime frontal rain, the corrections reduced the RMS difference by 62%.

Figure 7. Similar to Fig 6 but for a period of frontal rain 1100-1530UTC on 16 Mar 1991. In this case, the corrections reduced the RMS difference by 60%.

Figure 8. The best estimate of the RMS error in surface precipitation rate derived from Wardon Hill radar data during 7 periods of frontal rainfall including those illustrated in Figs 6 and 7. The RMS error is plotted as a function of the mean equivalent precipitation rate in the Chilbolton comparison data. The open symbols are for the raw Wardon Hill data and the closed symbols for the corrected data. Some cases were repeated using Wardon Hill data from higher elevation beams which presents a more severe test of the correction method.

Figure A1. The RMS difference between raw Wardon Hill radar measurements of reflectivity factor

(expressed as an equivalent precipitation rate) and simulations of the measurements from convolution of the beam power profile with a reflectivity factor profile derived from Chilbolton RHI data. The simulations were repeated using different assumed offsets between the nominal Wardon Hill beam elevation angles and the true elevation angles. The crosses are for the Wardon Hill beam with nominal elevation angle of 1.0 deg and the circles for the beam with nominal angle 0.5 deg.

Figure A2. A comparison between observed and simulated Wardon Hill radar precipitation rate measurements for the period 1100-1530UTC on 16 Mar 1991. The simulation used the best estimate of the true elevation angle of the lowest Wardon Hill beam (nominal angle = 0.5 deg).

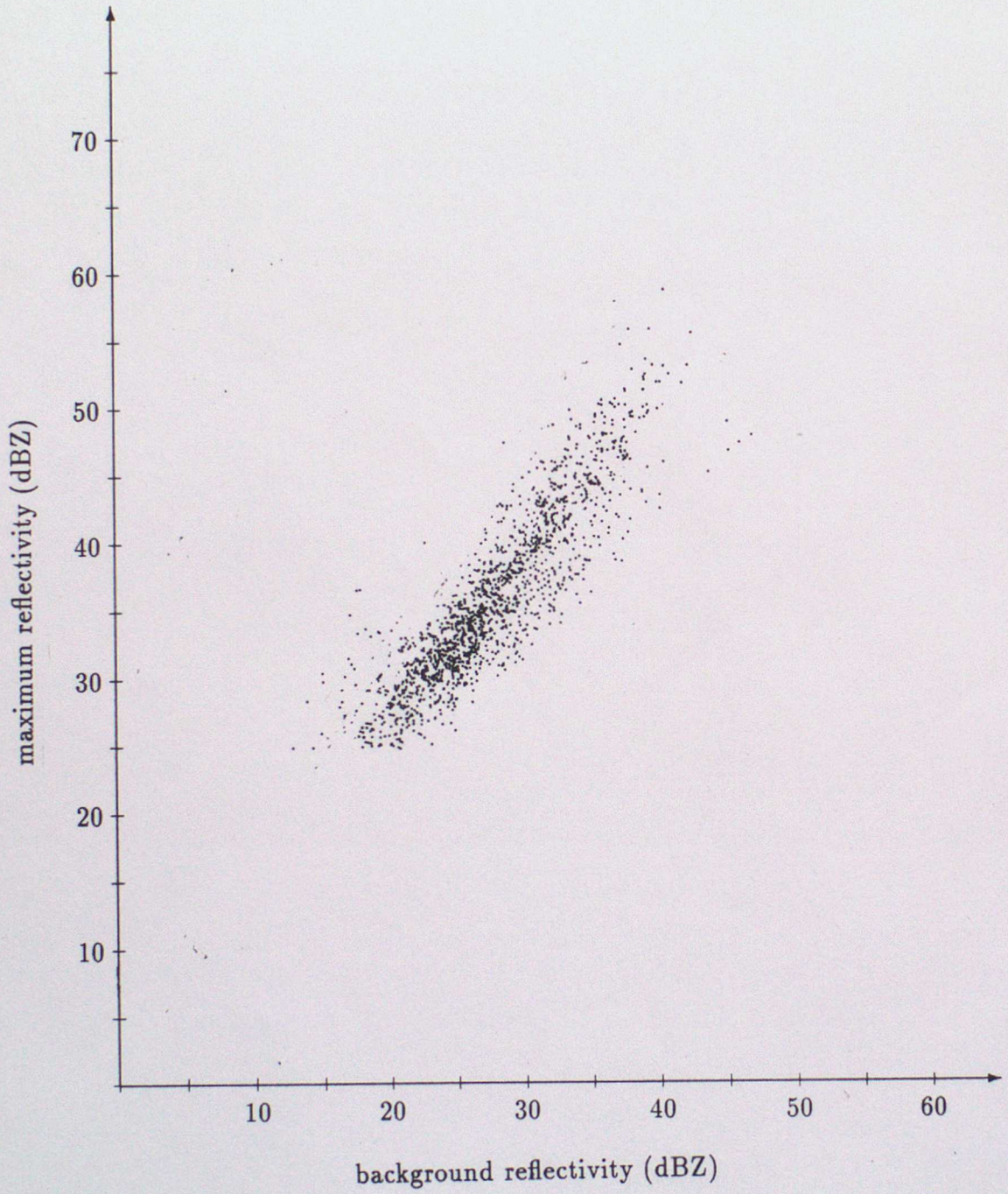

Figure 1. Scatter plot showing the relationship between the peak reflectivity factor measured in the bright band and the reflectivity factor in the rain beneath the bright band (the 'background' reflectivity factor, defined in the text). The data are from 1524 profiles of reflectivity factor recorded in widespread precipitation from stratiform cloud.

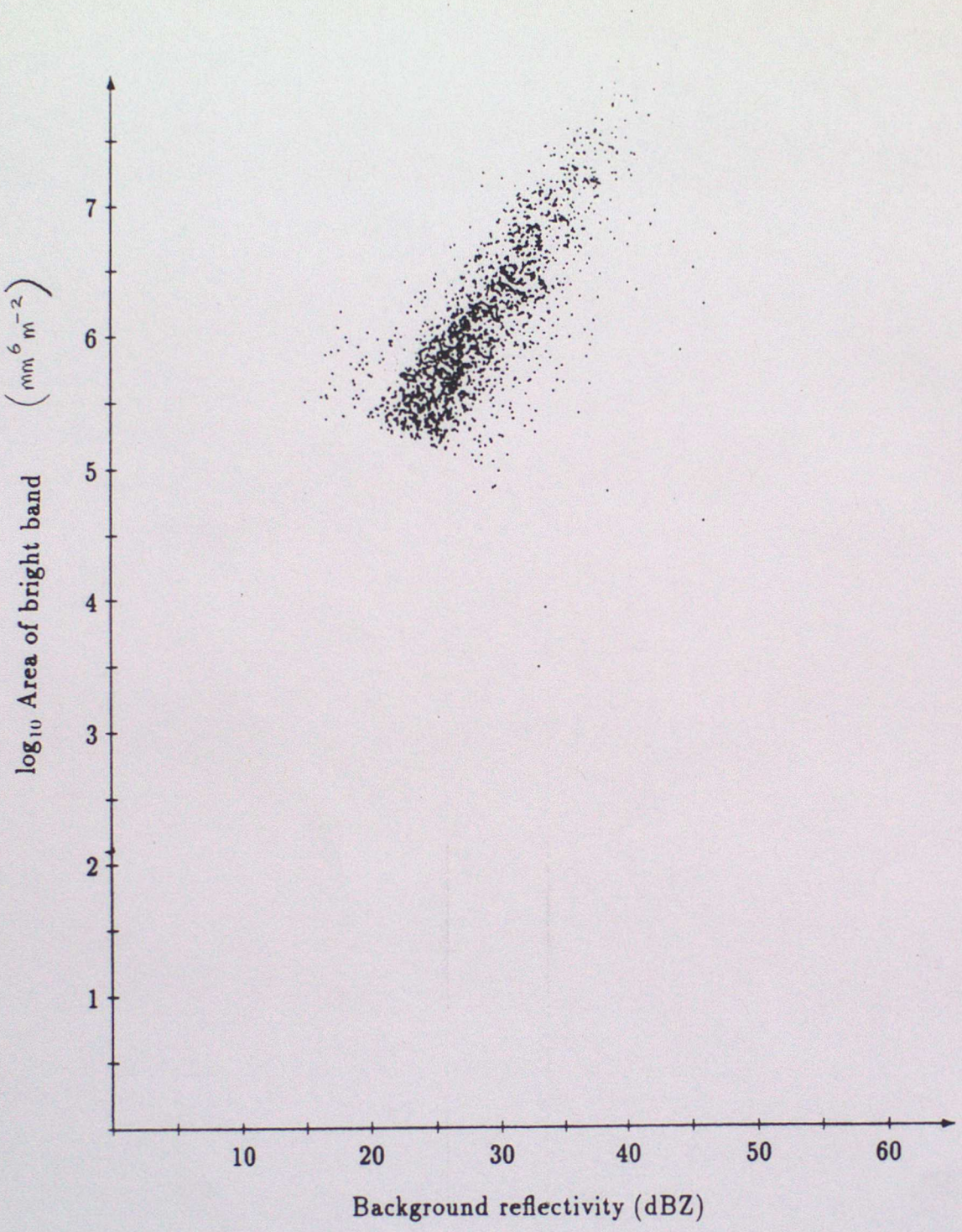

Figure 2. The area of the bright band peak as a function of the background reflectivity factor. The profile dataset was the same as that used in Fig 1.

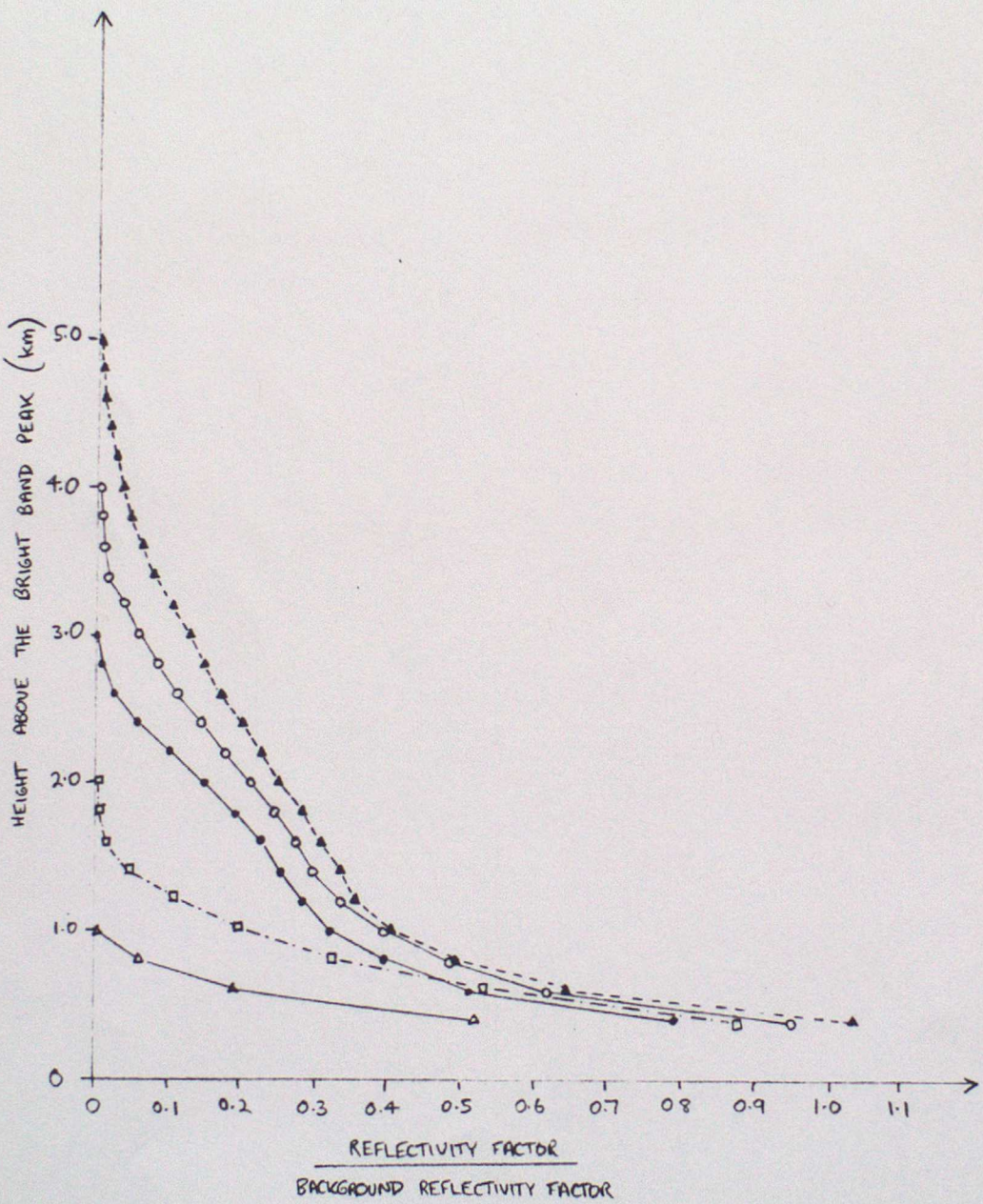

Figure 3. Results of analysis of reflectivity profiles within the snow above the melting layer. The reflectivity profiles were grouped into bands according to the separation distance between the height of the bright band peak and the top of the precipitation layer. The closed triangles are for separations 4-5km; the open circles, 3-4km; the closed circles, 2-3km; the open squares, 1-2km and the open triangles, 0-1km. The points on the curves represent the average ratio between the measured reflectivity factor at that level to the background reflectivity factor.

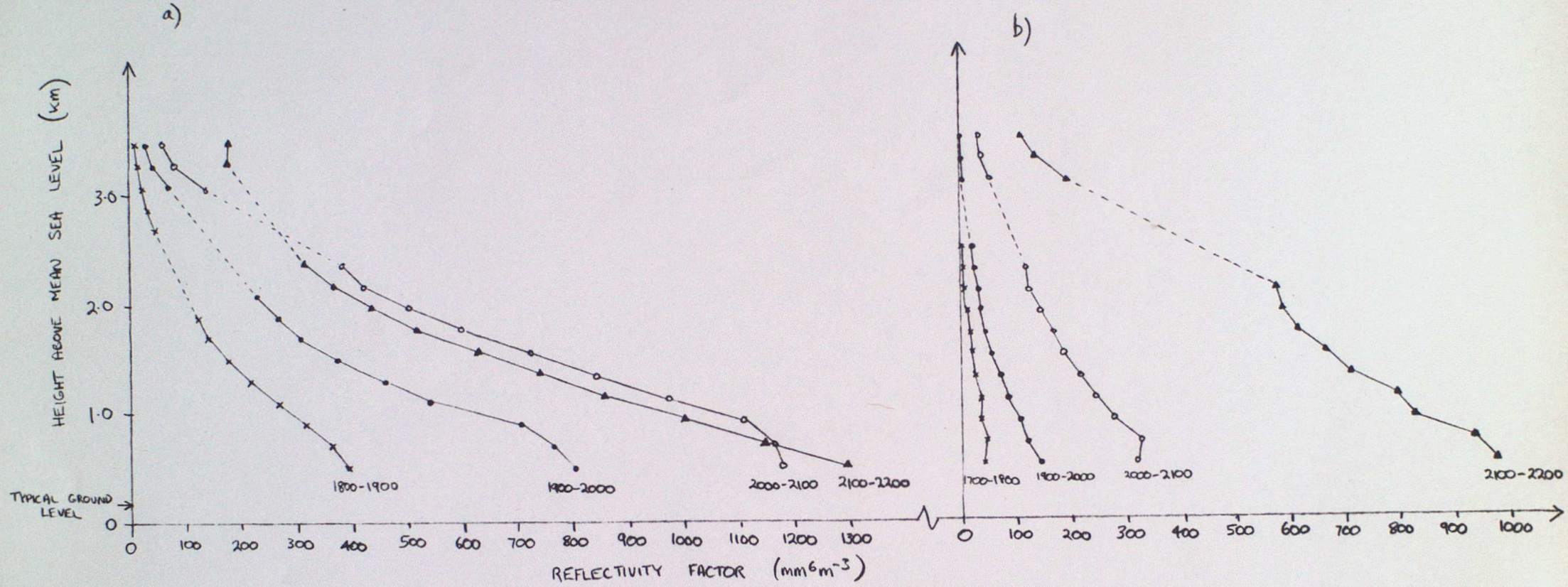

Figure 4. Hourly average reflectivity factor profiles recorded in two cases with low-level growth of precipitation; a) 20th Oct 1989 and b) 19th Oct 1989. The dashed portion of each profile is where the bright band peak has been omitted for clarity. The numbers at the base of each profile indicate the averaging period (UTC).

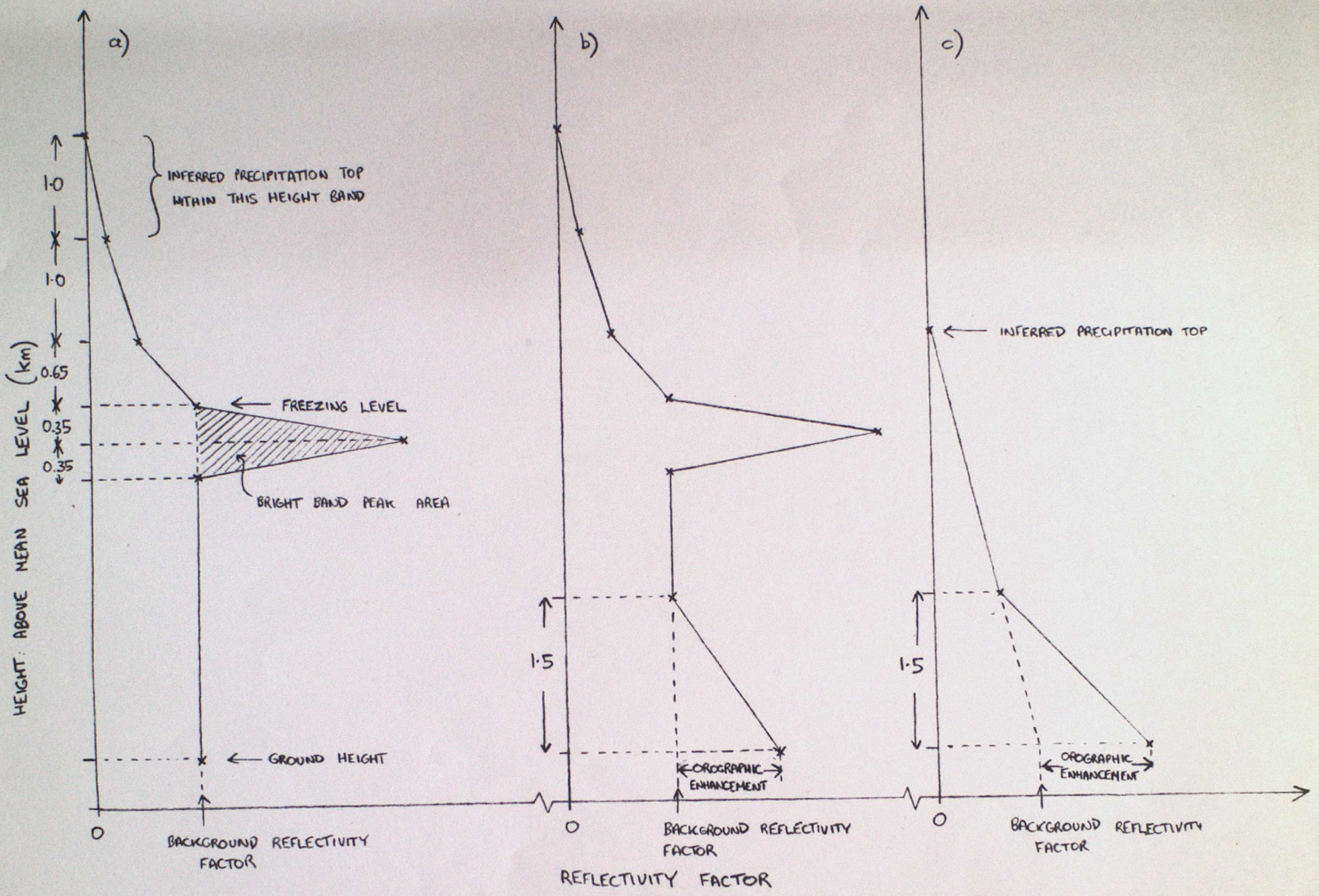

Figure 5. Examples of the construction of the idealized reflectivity factor profiles used in the correction method. a) is the most common case where no low-level orographic growth is diagnosed and the melting layer is within the precipitation layer. b) is similar to a) but with orographic growth. c) shows the simplified profile adopted when the surface temperature is less than 0 deg C and the precipitation is assumed to be snow.

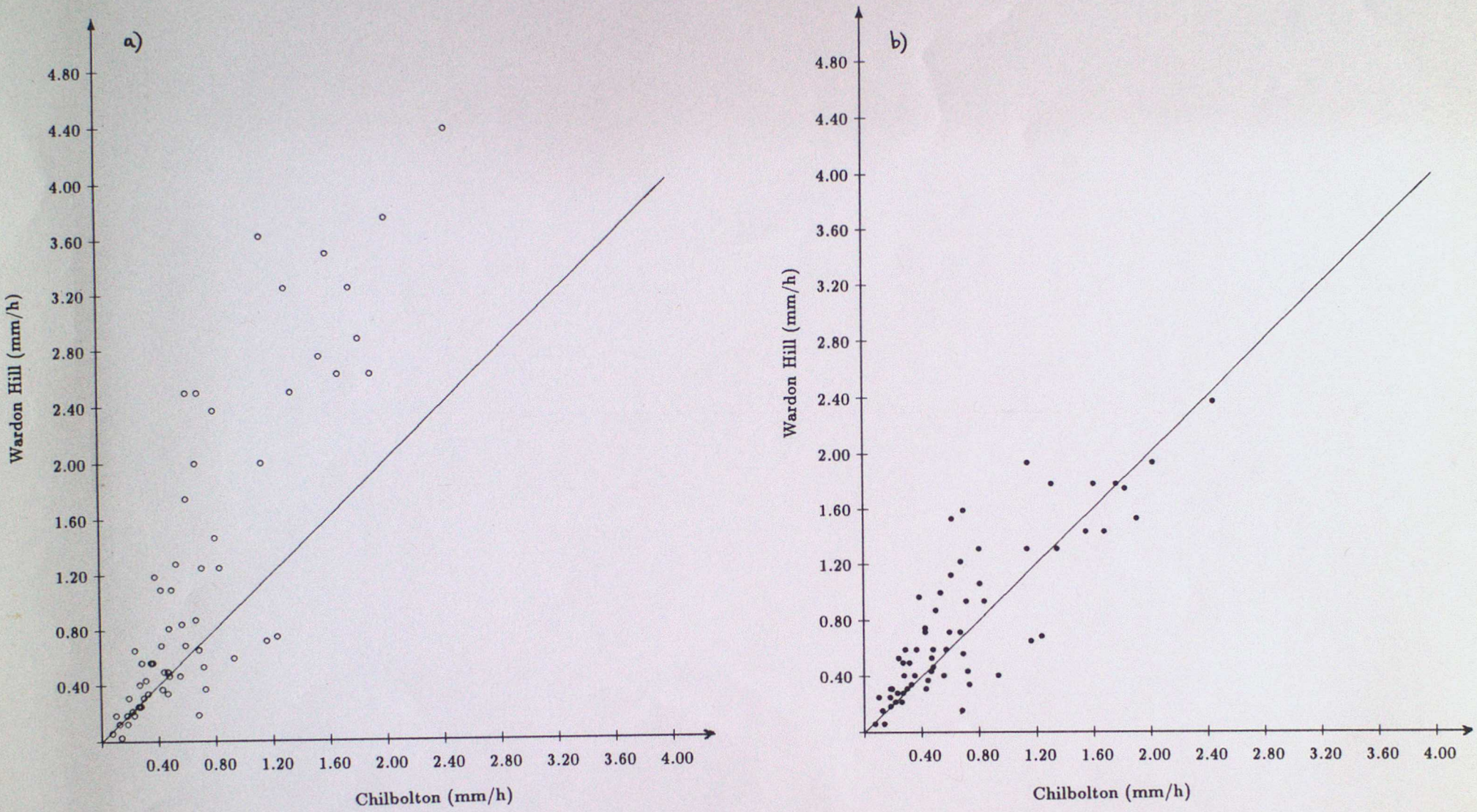

Figure 6. Example of the results of comparison between collocated measurements of instantaneous rainfall rate by the Wardon Hill operational weather radar and near-surface precipitation rate estimates derived from Chilbolton radar RHI data within the same 5km pixels. The time period for the comparison was 1500-1800UTC on 21 Feb 1991. a) is for the 'raw' Wardon Hill data and b) is for the same data corrected using the new method. In this case of typical wintertime frontal rain, the corrections reduced the RMS difference by 62%.

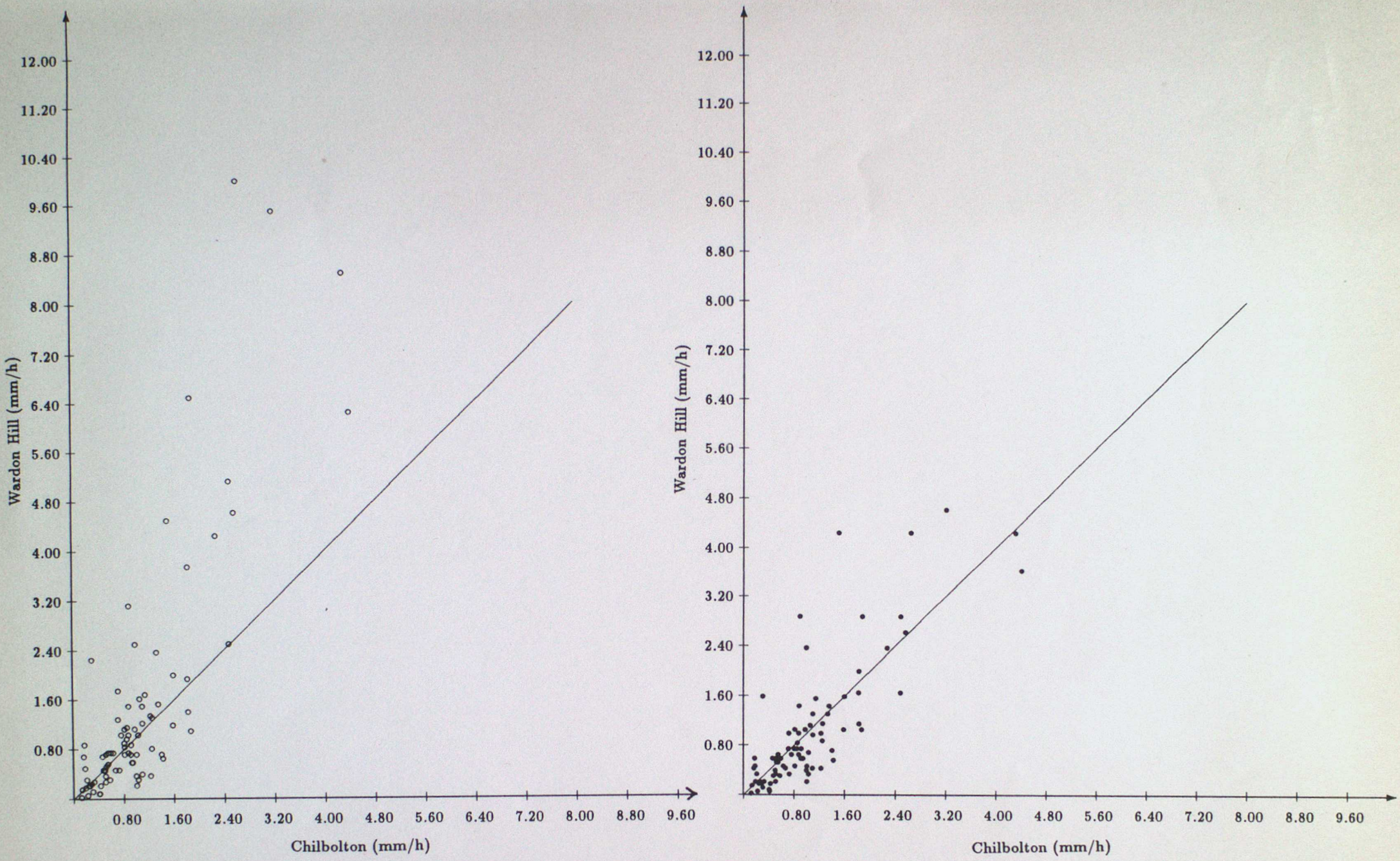

Figure 7. Similar to Fig 6 but for a period of frontal rain 1100-1530UTC on 16 Mar 1991. In this case, the corrections reduced the RMS difference by 60%.

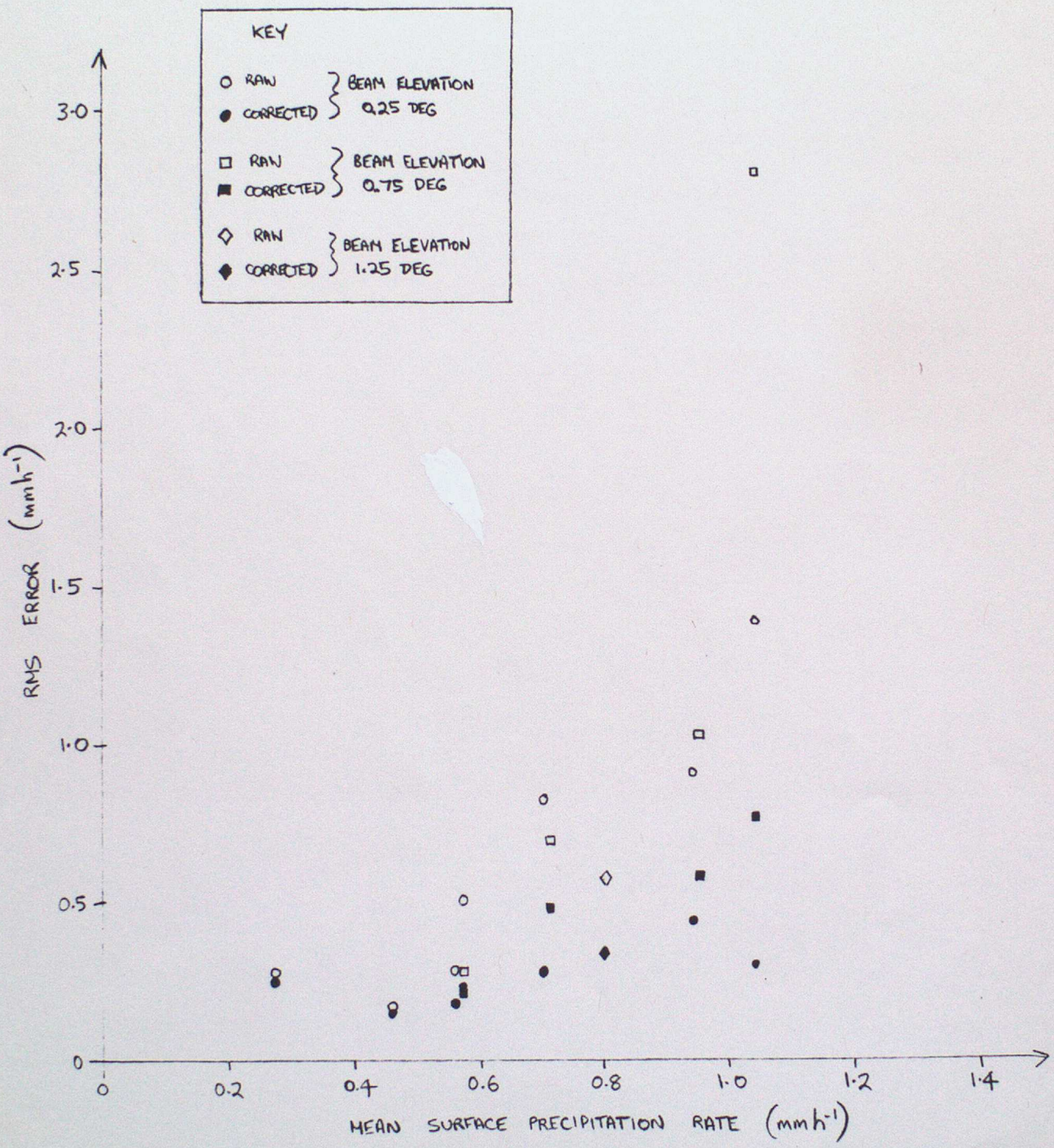

Figure 8. The best estimate of the RMS error in surface precipitation rate derived from Wardon Hill radar data during 7 periods of frontal rainfall including those illustrated in Figs 6 and 7. The RMS error is plotted as a function of the mean equivalent precipitation rate in the Chilbolton comparison data. The open symbols are for the raw Wardon Hill data and the closed symbols for the corrected data. Some cases were repeated using Wardon Hill data from higher elevation beams which presents a more severe test of the correction method.

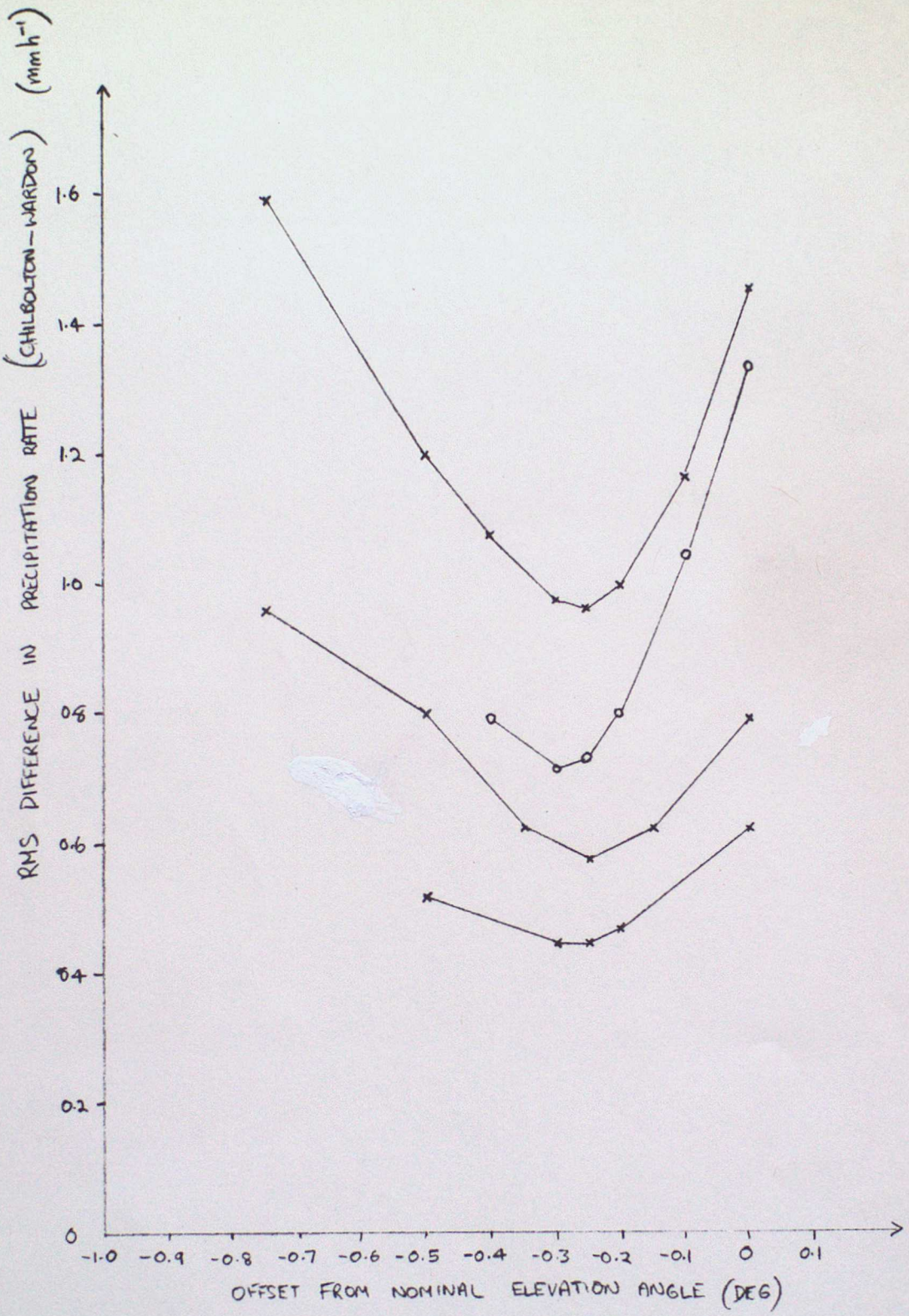

Figure A1. The RMS difference between raw Wardon Hill radar measurements of reflectivity factor (expressed as an equivalent precipitation rate) and simulations of the measurements from convolution of the beam power profile with a reflectivity factor profile derived from Chilbolton RHI data. The simulations were repeated using different assumed offsets between the nominal Wardon Hill beam elevation angles and the true elevation angles. The crosses are for the Wardon Hill beam with nominal elevation angle of 1.0 deg and the circles for the beam with nominal angle 0.5 deg.

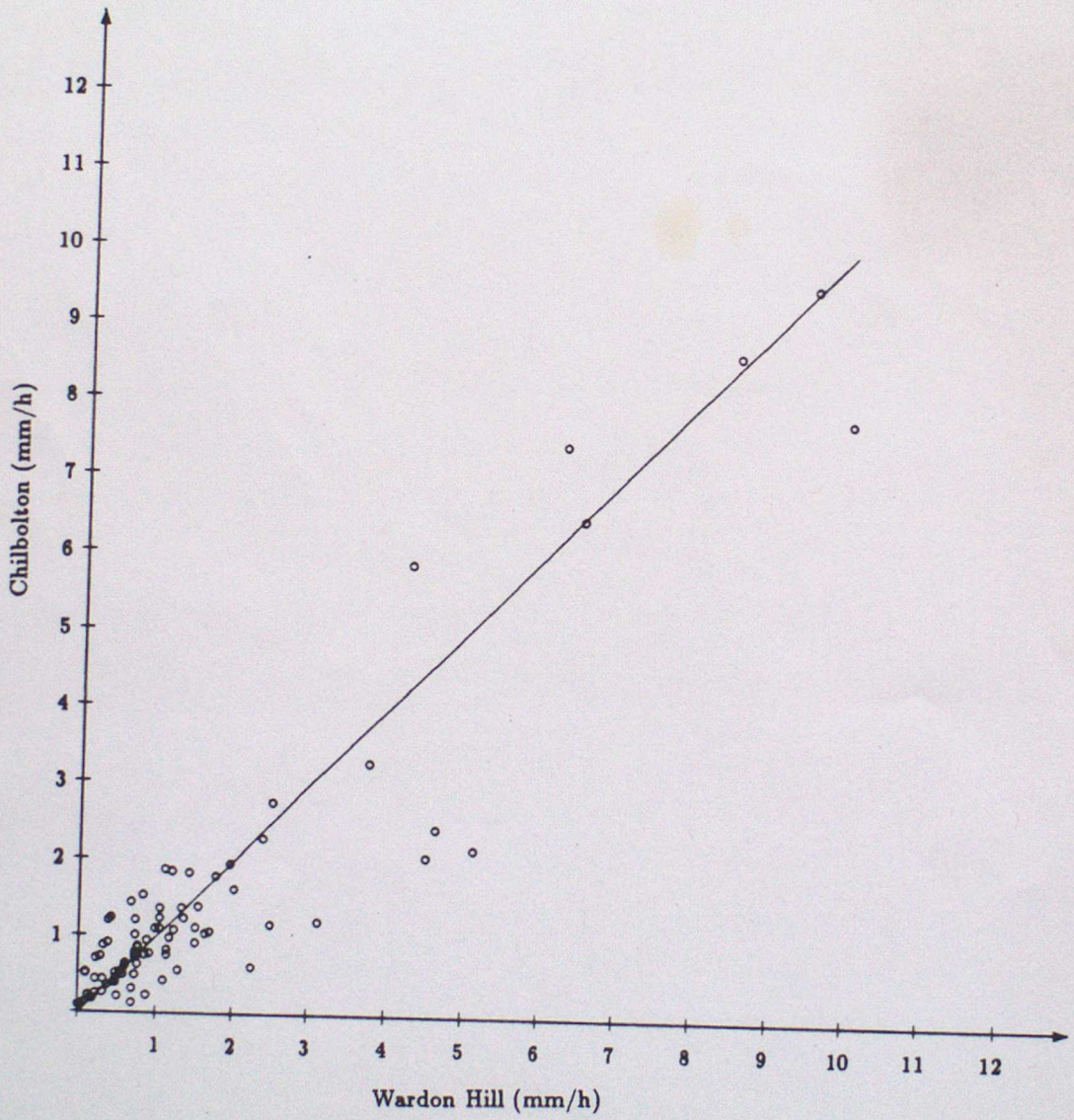

Figure A2. A comparison between observed and simulated Wardon Hill radar data for the period 1100-1530UTC on 16 Mar 1991. The simulation used the best estimate of the elevation angle of the lowest Wardon Hill beam (0.25 deg).

FORECASTING RESEARCH DIVISION SCIENTIFIC PAPERS

This series of Forecasting Research Division (FR) Scientific Papers . will be papers from all three sections of the Forecasting Research Division i.e. Data Assimilation Research (DA),Numerical Modelling Research (NM), and Observations and Satellite Applications (OB) the latter being formerly known as Nowcasting (NS). This series succeeds the series of Short Range Forecasting Research /Met O 11 Scientific Notes.

1. **THE UNIFIED FORECAST /CLIMATE MODEL .**
   M.J.P. Cullen
   September 1991

2. **Preparation for the use of Doppler wind lidar information in meteorological data assimilation systems**
   A.C. Lorenc, R.J. Graham, I. Dharssi, B. Macpherson, N.B. Ingleby, R.W. Lunnon
   February 1992

3. **Current developments in very short range weather forecasting.**
   B.J. Conway
   March 1992

4. **DIAGNOSIS OF VISIBILITY IN THE UK MET OFFICE MESOSCALE MODEL AND THE USE OF A VISIBILITY ANALYSIS TO CONSTRAIN INITIAL CONDITIONS**
   S.P. Ballard, B.J. Wright, B.W. Golding
   April 1992

5. **Radiative Properties of Water and Ice Clouds at Wavelengths Appropriate to the HIRS Instrument**
   A.J. Baran and P.D. Watts
   2nd June 1992

6. **Anatomy of the Canonical Transformation**
   M.J. Sewell and I. Roulstone
   27 June 1992

7. **Hamiltonian Structure of a Solution Strategy for the Semi-Geostrophic Equations**
   I. Roulstone and J. Norbury
   29 June 1992

8. **Assimilation of Satellite Data in models for energy and water cycle Research**
   A.Lorenc
   July 1992

9. **The use of ERS-1 data in operational meteorology**
   A.Lorenc, R.S.Bell, S.J.Foreman, M.W.Holt, D.Offiler C.D.Hall, D.L.Harrison, S.G.Smith
   August 1992

10. **Bayesian quality control using multivariate normal distributions**
    N.B. Ingleby and A. Lorenc
    July 1992

11. **A NEW APPROACH TO SHALLOW FLOW OVER AN OBSTACLE**
    I General Theory
    A.S. Broad, D. Porter and M.J. Sewell
    10 August 1992

12. **A NEW APPROACH TO SHALLOW FLOW OVER AN OBSTACLE II Plane Flow over a Monotonic Mountain**
A.S. Broad, D. Porter and M.J. Sewell
10 August 1992

13. **A Balanced Ocean Model with Outcropping**
Paul Cloke and M.J.P.Cullen
August 1992

14. **OSCILLATIONS IN THE ATMOSHERE'S ANGULAR MOMENTUM AND TORQUES ON THE EARTH'S BULGE**
M.J. Bell September 1992

15. **Preliminary assessment and use of ERS-1 altimeter wave data**
S.J.Foreman, M W Holt and S Kelsall
November 1992

16. **NON-GAUSSIAN PROBABILITIES IN DATA ASSIMILATION AND QUALITY CONTROL DECISIONS**
Andrew C Lorenc
November 1992

17. **Precipitation estimation with AVHRR data: a review**
G.L. Liberti
February 1993

18. **REAL-TIME CORRECTION OF WEATHER RADAR DATA FOR THE EFFECTS OF BRIGHT BAND, RANGE AND OROGRAPHIC GROWTH**
M.Kitchen, R Brown and A G Davies
July 1993